HHS Public Access

Author manuscript

ACS Infect Dis. Author manuscript; available in PMC 2019 April 25.

Published in final edited form as:

ACS Infect Dis. 2019 April 12; 5(4): 582–591. doi:10.1021/acsinfecdis.8b00321.

Combining 25-Hydroxycholesterol with an HIV Fusion Inhibitor Peptide: Interaction with Biomembrane Model Systems and Human Blood Cells

Bárbara Gomes[†], **Giusepinna Sanna**[‡], **Silvia Madeddu**[‡], **Axel Hollmann**[§,‖], and **Nuno C. Santos**[*,†]

[†]Instituto de Medicina Molecular, Faculdade de Medicina, Universidade de Lisboa, Lisbon 1649-028, Portugal

[‡]Department of Biomedical Sciences, Section of Microbiology and Virology, University of Cagliary, Cagliari 09123, Italy

[§]Laboratory of Bioactive Compounds, CIBAAL−University of Santiago del Estero and CONICET, Santiago del Estero, Argentina

[‖]Laboratory of Molecular Microbiology, Institute of Basic and Applied Microbiology, University of Quilmes, Bernal B1876BXD, Argentina

Abstract

The fusion between the viral and the target cell membrane is a crucial step in the life cycle of enveloped viruses. The blocking of this process is a well-known therapeutic approach that led to the development of the fusion inhibitor peptide enfuvirtide, clinically used against human immunodeficiency virus (HIV) type 1. Despite this significant advance on viral treatment, the appearance of resistance has limited its clinical use. Such a limitation has led to the development of other fusion inhibitor peptides, such as C34, that present the same structural domain as enfuvirtide (heptad repeat sequence) but have different functional domains (pocket-binding domain in the case of C34 and lipid-binding domain in the case of enfuvirtide). Recently, the antiviral properties of 25-hydroxycholesterol were demonstrated, which boosted the interest in this oxysterol. The combination of two distinct antiviral molecules, C34 and 25-hydroxycholesterol, may help to suppress the emergence of resistant viruses. In this work, we characterized the interaction of the C34−25-hydroxycholesterol conjugate with biomembrane model systems and human blood cells. Lipid vesicles and monolayers with defined lipid compositions were used as biomembrane model systems. The conjugate interacts preferentially with membranes rich in sphingomyelin (a lipid enriched in lipid rafts) and presents a poor partition to membranes composed solely of phosphatidylcholine and cholesterol. We hypothesize that cholesterol causes a repulsive effect that is overcome in the presence of sphingomyelin. Importantly, the peptide shows a preference for human peripheral blood mononuclear cells relative to erythrocytes, which shows its potential to target $CD4^+$ cells. Antiviral activity results against different wild-type and drug-

[*]**Corresponding Author:** Tel.: +351-217999480. Fax: +351-217999477. nsantos@fm.ul.pt.

Notes

The authors declare no competing financial interest.

resistant HIV strains further demonstrated the potential of C34-HC as a good candidate for future studies.

Graphical Abstract

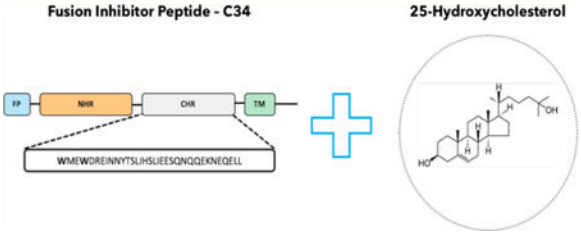

Keywords

human immunodeficiency virus; fusion; peptide; C34; 25-hydroxycholesterol

Yearly, human immunodeficiency virus type 1 (HIV-1) infections cause up to one million deaths worldwide.[1] Despite the declining incidence in the past few years, the displayed number is still alarmingly high and no cure or vaccine has been developed yet.

The entry of enveloped viruses on target cells is based on the binding and fusion between viral and target cell membranes.[2] In the case of HIV-1, the entry mechanism relies on the viral envelope glycoproteins complex formed by the transmembrane protein gp41 and the surface protein gp120. The process starts with gp120 binding to the CD4 receptor from T-lymphocytes, macrophages, and other immune system cells, which leads to a conformational change in gp120, allowing its contact with a coreceptor (CCR5 or CXCR4).[2–5] gp41 comprises a cytoplasm domain (CT), a transmembrane domain (TM), and an extracellular domain (ectodomain), which includes three major functional regions: fusion peptide (FP), N-terminal heptad repeat (NHR), and C-terminal heptad repeat (CHR).[6–8] The gp120 association with the coreceptor triggers a conformational change in gp41 and the insertion of the fusion peptide into the target cell membrane.[7,9,10] The two heptad repeats fold into each other creating a hairpin structure (or six helix bundle) that mediates an approach of the two membranes and promotes the formation of the fusion pore and viral content entry into the target cell.[7,8,11]

The use of peptides with an HR region corresponding sequence is therapeutically useful, since the peptide can bind to the prehairpin intermediate and prevent its transition to the hairpin structure, thereby blocking the fusion process.[12–14] The described therapeutic strategy culminated with the development of enfuvirtide (also known as T20 or Fuzeon), a fusion inhibitor peptide against HIV-1 clinically approved in 2003.[15] However, the drug is given subcutaneously, which leads to a poor therapeutic compliance, and it shows undesirable pharmacokinetics properties, such as low solubility and stability. Moreover, the use of enfuvirtide is associated with the development of drug resistance. In fact, Baldwin et al. described the appearance of an HIV-1 strain that requires enfuvirtide to fuse within the host cell.[16] Several approaches have been made to generate improved drug candidates.[12,17–19]

In this context, C34 was developed, a synthetic peptide based on the gp41 CHR region with 34 amino acid residues that blocks the formation of the fusogenic hairpin.[8,18] Contrarily to enfuvirtide, C34 does not present a lipid-binding domain, showing a weaker interaction with membranes. Such a limitation was overcome with the introduction of a cholesterol (Chol) moiety, which increased the antiviral potency, yielding a 50-fold decrease in peptide concentration blocking 50% of fusion (IC_{50}) (HXB2 strain) relative to C34 alone.[18,20] The introduction of sterol moieties and other peptide engineering strategies was also applied to other CHR-derived peptides, as entry inhibitors targeting paramyxoviruses.[19,21–23] It was expected that C34 could overcome viral resistance, since it has the hydrophobic residues W117, W120, and I124 that are highly conserved.[8,24,25] However, *in vitro* selection studies with C34 demonstrated that this peptide also leads to HIV-1 resistance, due to mutations on the gp41 N-terminal domain, specifically a leucine to serine substitution at position 33 and a valine to glutamic acid change at position 38.[26]

In parallel with those findings, a sterol derived from cholesterol, 25-hydroxycholesterol (25HC), was shown to be an efficient antiviral molecule, with a high potency to inhibit a broad spectrum of viruses at high to low concentrations, depending on lipid conditions and the virus−host cell system.[27–30] At the cellular level, 25HC is enzymatically synthesized from cholesterol by a nonheme, iron containing protein, cholesterol-25-hydroxylase (Ch25h).[31] Liu et al. demonstrated that both 25HC and Ch25h are capable of inhibiting HIV entry at the membrane level.[27] Indeed, our recent work has shown that 25HC directly prevents the fusion process through the modification of lipid membrane properties and by alterations on HIV-fusion peptide conformational plasticity.[32] These results corroborate the broad-spectrum antiviral activity of 25HC.

Combining the fusion inhibitor peptide C34 with the antiviral sterol 25HC (referred to as C34-HC) may be an alternative strategy in HIV therapy. On one hand, the resistance promoted by the peptide can be overcome by combining two molecules with different targets, the viral protein gp41 and the viral membrane;[33] on the other hand, the use of a peptide specific for HIV makes the effect of 25HC more precise.

We have previously shown that the biophysical properties of fusion inhibitor peptides are crucial for their interaction with cell and viral membranes, which as a consequence can modify their antiviral activity.[22,23,34,35] With this work, we intended to characterize the interaction of C34-HC with biomembranes. Using large unilamellar vesicles (LUVs) and lipid monolayers as membrane model systems and human blood cells as a biological model, we performed a detailed study to elucidate the peptide−membrane interaction. Finally, we evaluated the antiviral activity of this peptide against wild-type (wt) and different drug-resistant HIV strains, comparing the data with that obtained for enfuvirtide. The antiviral potency of C34-HC was determined not only to validate the peptide conjugate as an alternative to enfuvirtide but also to assess its broad-spectrum activity against different viral strains.

RESULTS AND DISCUSSION

Membrane Partition.

Addition of 25HC to the peptide backbone promotes a blue shift on the C34 spectra (Figure 1), which indicates a change in the tryptophan (Trp) surrounding microenvironment.[34]

In order to quantify the extent of interaction of the peptides with the LUV membranes (Table 1), the partition coefficient between the lipid and aqueous phases, K_p, was determined by using eq 1 to fit the fluorescence intensity data (Figure 2).

With pure POPC (1-palmitoyl-2-oleoyl-*sn*-glycero-3-phosphocholine) vesicles, the K_p value obtained was 1543 ± 347, which indicates a significant interaction between the lipid and the peptide.

The lowest Kp value was obtained in the presence of the POPC:Chol membranes (516 ± 90) which could indicate a “repulsive” action induced by the presence of cholesterol on the membrane composition. Nonetheless, when sphingomyelin (SM) is also present, the interaction increases, which establishes the importance of having both cholesterol and sphingomyelin in the membrane. Such an observation is particularly relevant since both lipids are highly concentrated in lipid rafts, the major platforms for viral fusion.[36–38]

Finally, for the HIV-like mixture, the partition coefficient reaches values similar to those found for pure POPC. This behavior is opposite to the one displayed by C34-cholesterol, which shows a preference for cholesterol-rich membranes.[20] This difference between the two molecules confirms that the interaction between peptides and biomembranes depends not only on the presence but also on the type of lipid moiety used.

Surface Pressure Perturbation of Monolayers.

From the partition results, we observed that C34-HC seems to interact better with pure POPC lipid membranes, comparatively to POPC:Chol (2:1) vesicles. However, due to the terminal position of the Trp residues in this peptide sequence, one cannot discard the hypothesis that the peptides may be interacting with membranes, leaving its two Trp residues fully exposed to the aqueous environment, without changes in the quantum yield (therefore, not influencing the K_p calculation). Surface pressure measurements on POPC and POPC:Chol (2:1) monolayers were carried out, using a low initial surface pressure (20.5 mN/m). Usually, the adsorption and penetration of molecules is favored at a low surface density (loosely packed lipid monolayers), whereas high surface pressures (compact lipid packing) hinder the penetration in the lipid monolayers. Control experiments were carried out using only DMSO (solvent), and no significant changes were observed. K_d and $\Delta\Pi_{max}$ values were determined by fitting the experimental data with eq 2 in order to quantify the interaction of C34-HC in the Langmuir monolayers.

In the pressure studies, it was possible to observe that C34-HC has a higher affinity for pure POPC membranes (K_d = 0.1008 ± 0.0082 μM) comparatively to POPC:Chol (2:1) (K_d = 0.2484 ± 0.0548 μM) (Figure 3). This is in good agreement with the data obtained on the partition studies.

Localization in the Lipid Bilayer.

The accessibility of the fluorophores to the aqueous environment was studied through the fluorescence quenching of the Trp residues of the peptide by acrylamide. Acrylamide is a water-soluble quencher, with low capacity for penetration into lipid bilayers. It is generally used to assess the aqueous environment accessibility of the Trp residues in the peptide structure and infer on their insertion on lipid bilayers.[39] When the peptide is inserted in a lipid membrane, it becomes less accessible to the quencher present in the solution and, consequently, its fluorescence will be less quenched by acrylamide. Linear Stern−Volmer plots were obtained in the presence of different lipid compositions tested (Figure 4).

For C34-HC, all the assays with lipids yielded K_{SV} values lower than those obtained in their absence (9.48 ± 0.36 mM^{-1} with buffer, 5.57 ± 0.32 mM^{-1} in the presence of POPC, 4.57 ± 0.36 mM^{-1} for POPC:Chol vesicles, 6.95 ± 0.85 mM^{-1} in the presence of POPC:Chol:SM vesicles, and 7.45 ± 0.28 mM^{-1} in the presence of the HIV-like mixture). These reductions on the Stern−Volmer constant, but keeping a linear Stern−Volmer plot, indicate that the interaction with the membrane occurs with the fluorophores partially exposed to the aqueous environment.

Fluorescence quenching measurements were also used to estimate the depth of insertion of the Trp residues of the peptide in POPC, POPC:Chol (2:1), and HIV-like mixture membranes. Stearic acid molecules derivatized with doxyl (quencher) groups at either carbon 5 (5NS) or 16 (16NS) were used for this purpose. 5NS is a better quencher for molecules inserted in the membrane in a shallow position, close to the lipid−water interface, while 16NS is better for molecules buried deeply in the membrane.[40] Figure 5A shows the plot obtained for C34-HC on POPC, POPC:Chol (2:1), and the HIV-like mixture using the effective concentration of 5NS and 16NS in the bilayer matrix.[40]

For POPC, the K_{SV} with 5NS was higher (3.71 ± 0.36 mM^{-1}) than for 16NS (1.43 ± 0.31 mM^{-1}). The same trend was observed in the case of POPC:Chol (2:1): the K_{SV} for 5NS (6.25 ± 0.32 mM^{-1}) was also higher than for 16NS (2.69 ± 0.16 mM^{-1}).

As observed in the presence of POPC and cholesterol, the peptide seems to be located in a more superficial position and more exposed to the aqueous media. When in pure POPC LUVs, C34-HC is located closer to the center of the bilayer. The same behavior was observed for C34-cholesterol, although for that molecule the difference between the two lipid compositions was not so evident (16.8 Å away from the center of the bilayer for POPC and 18 Å for POPC:Chol 2:1).[20] The higher difference observed for C34-HC corroborates the hypothesis that cholesterol decreases the insertion of the peptide due to the presence of another sterol, an effect that seems to be overcome when sphingomyelin is present. Interestingly, using an HIV membrane-like mixture, the peptide inserts deeply into the bilayer, closer to its center. We hypothesize that the peptide inserts on the viral membrane, probably being carried with the virus to the fusion site. This would improve the peptide's metabolic stability, decrease its clearance, and increase its half-life time, enhancing its availability at the required site of action.

Membrane Dipole Potential Assessment Using di-8-ANEPPS.

In order to complement the membrane partition assays, which only follow the peptide's Trp intrinsic fluorescence, peptide−membrane interaction was also evaluated using the lipophilic probe di-8-ANEPPS,[20,34] which is sensitive to the membrane dipole potential.[41] It was used to label lipid vesicles composed of POPC, POPC:Chol (2:1), POPC:Chol:SM (1:1:1), and the HIV membrane-like mixture (Figure 6A,B). If the peptide interacts by inserting or adsorbing on the membrane, it is expected that it changes the membrane dipole potential to some extent. These changes can be reported by the di-8-ANEPPS excitation spectrum. A shift to higher wavelengths (lower frequencies) indicates a decrease in the membrane dipole potential, whereas a shift to lower wavelengths corresponds to an increase in dipole potential,[41,42] becoming easier to assess in differential spectra. The fluorescence red-shift (i.e., higher wavelength) observed on the emission spectra of the di-8-ANNEPS probe indicates a decrease in the membrane dipole potential in a peptide concentration-dependent manner.

The peptide−membrane interaction was quantified by measuring the ratio (R) of intensities at the excitation wavelengths of 455 and 525 nm, with emission at 670 nm, for a range of peptide concentrations. R is a quantitative descriptor of spectral shifts and, hence, of the relative variation of dipole potential. The membrane dipole potential significantly decreased in the presence of C34-HC (Figure 6). Additions of DMSO or C34 (without sterol) were also tested as a control, and no changes on the dipole potential were observed (data not shown).

As shown in Table 2, the peptide exhibits a higher affinity for the HIV-like mixture followed by the canonic lipid raft composition (POPC:Chol:SM), which confirms the peptide affinity for mixtures of cholesterol and sphingomyelin and its possible interaction with viral membranes.

Although these results are not in agreement with the partition data, that showed a preference for POPC vesicles, it should be pointed out that in the partition assays only the local changes on the Trp microenvironment are monitored, whereas the dipole potential changes are able to assess the interaction of the whole fusion inhibitor with the membrane.

Interaction with Blood Cells.

After the characterization of the peptide−membrane interactions using membrane model systems, we studied this peptide−membrane interaction in biological settings, with isolated human erythrocytes and peripheral blood mononuclear cells (PBMCs), also labeled with the fluorescent probe di-8-ANEPPS. PBMCs are one of the HIV-1 main targets, but HIV-1 can also interact with the surface of erythrocytes, upon circulating on the bloodstream.[43–45]

C34-HC decreases the membrane dipole potential of both blood cell types, demonstrating its interaction with those cells (Figure 7). It is interesting to detect that the peptide interacts better with PBMCs (K_d = 0.25 ± 0.02 μM) than with erythrocytes (K_d = 0.43 ± 0.11 μM), in contrast with C34-cholesterol, which interacts with both cell types at the same extent.[20] This is in good agreement with the data obtained with LUVs, since the cholesterol/sphingomyelin ratio is higher in erythrocytes than in PBMCs.[46] While for erythrocytes cholesterol represents 50% of the total lipids at the membrane level and sphingomyelin just 15%, in the

case of PBMCs, cholesterol is between 20% and 25% (depending on the type of cells, monocytes or lymphocytes) and sphingomyelin is between 10% and 15%.[46]

Antiviral Activity.

Table 3 shows the peptide concentrations necessary to achieve 50% (IC_{50}) or 90% (IC_{90}) protection of MT-4 cells from HIV-1 induced cytopathogenicity, as well as the required concentrations to reduce the viability of mock-infected cells by 50% (CC_{50}). In our *in vitro* assay, C34-HC was more effective against all the HIV-1 strains tested than enfuvirtide, the only fusion inhibitor peptide approved by FDA. The conjugate C34-HC is also more effective than C34 (IC_{50} = 1.4 nm), as described in the literature.[47]

When tested against the HIV-1_{IIIB} strain (wild-type virus), C34-HC presents an IC_{50} 25 times lower and an IC_{90} 40 times lower than enfuvirtide. The same trend was observed against non-nucleoside reverse transcriptase inhibitor (NNRTI)-resistant and nucleoside reverse transcriptase inhibitor (NRTI)-resistant mutants, always with IC_{50} on the subnanomolar range, demonstrating its broad-spectrum activity against different viral strains. The NRTI-resistant strain combines four mutations that confer the virus resistance to zidovudine, also known as azidothymidine (AZT), the first treatment for HIV.[48] The mutations studied developed with the use of NNRTIs were the Y181C, Y181C + K103N, and the triple mutant K103R + V179D + P225H (resistant to efavirenz, EFV), which are critical for the binding of the NNRTIs to the retroviral reverse transcriptase.[49]

CONCLUSION

Despite the interest and enthusiasm with enfuvirtide approval by FDA, no other fusion inhibitor peptide was able to reach the pharmaceutical market. Moreover, this commercialized peptide presents some disadvantages such as undesired pharmacokinetic properties and the appearance of resistant strains, and it is an option just as a combined therapy. The plasticity of HIV-1 and the capacity to acquire mutations suggest that the combination of drugs with different targets is the best way to mitigate the risk of resistance.

In parallel, the observation that 25HC, a cholesterolderivative, is a broad-spectrum antiviral molecule,[27,32] opened a promising new antiviral strategy. We have shown that 25HC is able to directly block fusion between membranes.[32] We hypothesize that replacement of cholesterol by 25HC at the membrane level leads to a weaker effect of the HIV fusion peptide at the host cell.[32]

In this work, we studied the membranotropic properties of C34-HC, a well-known antiviral peptide, attached to 25HC, bearing in mind the advantages of having two different moieties working together for the same purpose but with different modes of action. We have previously shown that specific biophysical properties of virus-derived peptides modulate their interaction with biomembranes, which can in turn affect their antiviral potency.[22,23,34,35] In this work, we demonstrated that C34-HC interacts with membranes mimicking lipid rafts and has an increased affinity for PBMCs, which may indicate a selectivity for $CD4^+$ cells, the main target of HIV. This fact is of great importance, as binding selectivity is one of the key properties in drug development. The balance between narrow and broad

selectivity is a continuous challenge, and unexpected interactions can lead to undesired and severe side effects. Additionally, the peptide extensively interacts with vesicles mimicking the HIV membrane, which opens the possibility of being carried by the virus to its target.

Finally, C34-HC has a superior antiviral efficiency comparatively to enfuvirtide, the only HIV fusion inhibitor currently in clinical use. Different drug-resistant strains were also tested, demonstrating the ability of C34-HC to inhibit a broad panel of mutant viruses. The increasing levels of antimicrobial resistance, observed in the last years, are a serious threat to global public health with tremendous social and economic implications. The development of alternative solutions is therefore an urgent need. Hence, we consider C34-HC as a good candidate for further studies.

MATERIALS AND METHODS

Reagents.

The C34 sequence is WMEWDREINNYTSL-IHSLIEESQNQQEKNEQELL.[18] For C34-HC, it was con-jugated as C34-GSGC-25HC (American Peptide Company, Sunnyvale, CA, USA). 5NS (5-doxyl-stearic acid) and 16NS (16-doxyl-stearic acid) were from Aldrich (Milwaukee, WI, USA). L-Tryptophan (Trp), acrylamide, HEPES, and NaCl were from Merck (Darmstadt, Germany). POPC, DPPC (1,2-dipalmitoyl-*sn*-glycero-3-phosphocholine), SM, POPE (1-palmitoyl-2-oleoyl-*sn*-glycero-3-phosphoethanolamine), and POPS (1-palmitoyl-2-oleoyl-*sn*-glycero-3-phospho-$_L$-serine) were purchased from Avanti Polar Lipids (Alabaster, AL, USA), while cholesterol and Pluronic F-127 were from Sigma (St. Louis, MO, USA). Di-8-ANEPPS was from Invitrogen (Carlsbad, CA, USA), and Lymphoprep was from Stem Cell Technologies (Grenoble, France).

MT-4 and H9/III$_B$ cells were obtained from NIH AIDS Research & Reference Reagent Program, USA. Cell cultures were grown in RPMI 1640 medium, supplemented with 10% fetal calf serum (FCS), 100 IU/mL penicillin G, and 100 μg/ mL streptomycin and incubated at 37 °C in a 5% CO_2 atmosphere. Cell cultures were checked periodically for the absence of mycoplasma contamination with MycoTect Kit (Gibco, Waltham, MA, USA). HIV-1$_{IIIB}$ was obtained from supernatants of persistently infected H9/III$_B$. The Y181C mutant (NIH N119) derives from an AZT-sensitive clinical isolate passaged initially in CEM and then in MT-4 cells in the presence of nevirapine (up to 10 μM). The K103N + Y181C mutant (NIH A17) derives from a III$_B$ strain passaged in H9 cells in the presence of BI-RG 587 (up to 1 μM). The K103R + V179D + P225H mutant (EFV^R) derives from a III$_B$ strain passaged in MT-4 cells in the presence of efavirenz (up to 2 μM). A strain carrying mutations associated to NRTI resistance, AZT^R (67N, 70R, 215F, 219Q), was also tested.

Fluorescence Spectroscopy Measurements.

The presence of tryptophan residues on C34-HC allows the use of fluorescence spectroscopy techniques to study this molecule. The working buffer used throughout the studies was 10 mM, pH 7.4 HEPES in 150 mM NaCl. C34-HC (500 μM) stock solutions were prepared in DMSO. Trp (500 μM) stock solutions were prepared in buffer. Large unilamellar vesicles (LUVs) were prepared by extrusion methods, as described elsewhere.[50,51]

Membrane partition, fluorescence quenching studies using acrylamide, and membrane dipole potential characterization using di-8-ANEPPS were carried out in a Varian Cary Eclipse fluorescence spectrophotometer (Mulgrave, Australia) and time-resolved fluorescence spectroscopy studies in a LifeSpec II Fluorescence Lifetime spectrometer (Edinburgh Instruments, Livingston, UK).

The fluorescence spectral characterization of C34-HC and Trp was performed with an excitation wavelength of 280 nm, except for 5NS, 16NS, and acrylamide quenching experiments, where the excitation was performed at 290 nm to minimize the relative quencher/fluorophore light-absorption ratios. For the partition studies and the quenching experiments, fluorescence emission was collected from 310 to 450 nm as an integrated spectra. Typical spectral bandwidths were 5 nm for excitation and 10 nm for emission. Excitation and emission spectra were corrected for wavelength-dependent instrumental factors.[52] During the quenching and partition experiments, emission was also corrected for successive dilutions, scatter, and simultaneous light absorptions of quencher and fluorophore. All the fluorescence measurements in this study were performed at room temperature (approximately 25 °C).

Partition Coefficient Determination.

Membrane partition studies were performed by successive additions to a 5 μM C34-HC solution of small amounts of LUV suspensions with different lipid compositions, including: POPC, POPC:Chol (2:1), POPC:Chol:SM (1:1:1), and an HIV membrane-like mixture (5.3% POPC, 3.5% DPPC, 45.3% cholesterol, 18.2% SM, 19.3% POPE, and 8.4% POPS), with a 10 min incubation time between each addition. The partition coefficients (K_p) were calculated using the equation:[53]

$$\frac{I}{I_W} = \frac{1 + K_p \gamma_L \frac{I_L}{I_W}[L]}{1 + K_p \gamma_L [L]} \quad (1)$$

where I_W and I_L are the fluorescence intensities in aqueous solution and in lipid, respectively, γ_L is the molar volume of the lipid,[53–55] and $[L]$ is its concentration.

Surface Pressure.

Changes on the surface pressure of lipid monolayers induced by C34-HC were measured in an NIMA ST900 Langmuir−Blodgett Trough (Coventry, UK) at constant temperature (25 ± 0.5 °C). The surface of a HEPES buffer solution contained in a Teflon trough of fixed area was exhaustively cleaned by surface aspiration. Then, a solution of lipids in chloroform was spread on the air−water interface, reaching a surface pressure of 20.5 ± 1 mN/m. Peptide solutions were injected in the subphase, and the changes on the surface pressure were followed during the necessary time to reach a constant value. The surface pressure of the air −water interface upon injecting the largest concentration of each peptide used throughout the studies was always below 15 mN/m. For this reason, the lowest initial surface pressure of the lipid monolayers before the addition of the peptides to the subphase was above that value. In

these conditions, the changes in surface pressure observed upon the injection of the peptide can be attributed to an effect of the peptide on the monolayer interfacial tension. The dissociation constant (K_d) was calculated from the adsorption Langmuir isotherm:

$$\Delta\Pi = \frac{\Delta\Pi_{max}[\text{peptide}]}{K_d + [\text{peptide}]} \quad (2)$$

where $\Delta\Pi$ is the change of surface pressure, $\Delta\Pi_{max}$ is the maximum change of pressure achieved, and [peptide] is the peptide concentration.

Acrylamide Quenching.

The fluorescence quenching of 5 μM C34-HC by acrylamide (0−60 mM) was studied in buffer and in the presence of POPC, POPC:Chol (2:1), and a HIV-like mixture with 3 mM LUVs by successive additions of small volumes of the quencher stock solution.[39] For every addition, a minimal 10 min incubation time was allowed before measurement. Quenching data were analyzed by using the Stern−Volmer equation:[53]

$$\frac{I_0}{I} = 1 + K_{SV}[Q] \quad (3)$$

where I and I_0 are the fluorescence intensity of the sample in the presence and absence of quencher, respectively, K_{SV} is the Stern−Volmer constant, and [Q] the concentration of quencher.

5NS and 16NS Quenching.

Fluorescence quenching assays with the lipophilic probes 5NS and 16NS were performed by time-resolved fluorescence spectroscopy. These assays were carried out at the same peptide and lipid concentrations used for the acrylamide quenching, by successive additions of small amounts of these quenchers (in ethanol) to samples of peptide in POPC and POPC:Chol (2:1), keeping the ethanol concentration below 2% (v/v).[56] The effective lipophilic quencher concentration in the membrane was calculated from the partition coefficient of both quenchers to the lipid bilayers.[57] For every addition, a minimal 10 min incubation time was allowed before measurement. Quenching data were analyzed by using the Stern−Volmer equation (eq 3) or the Lehrer equation (eq 4)[57,58] when a negative deviation to the Stern −Volmer relationship is observed:

$$\frac{I_0}{I} = \frac{1 + K_{SV}[Q]}{(1 + K_{SV}[Q])(1 - f_b) + f_b} \quad (4)$$

where f_b is the fraction of light arising from the fluorophores accessible to the quencher. In the case of dynamic quenching, the relationship $I_0/I = \tau_0/\tau$ is valid; thus, time-resolved quenching data can be analyzed by using the same equations (eqs 3 and 4).

Membrane Dipole Potential Assessed by di-8-ANEPPS.

For lipid vesicles labeling, suspensions with 500 μM of total lipid were incubated overnight with 10 μM di-8-ANEPPS to ensure maximum incorporation of the probe. Human blood samples were obtained from healthy volunteers, with their previous written informed consent, at Instituto Portugueŝdo Sangue (Lisbon, Portugal), as approved by the Joint Ethics Committee of Faculdade de Medicina da Universidade de Lisboa and Centro Hospitalar Lisboa Norte. Isolation of erythrocytes and PBMCs and labeling of these cells with di-8-ANEPPS were performed as previously described.[59,60] For erythrocytes isolation, blood samples were centrifuged at 1200*g* during 10 min to remove plasma and buffy-coat. Remaining erythrocytes were washed twice in working buffer. They were then incubated at 1% hematocrit in buffer supplemented with 0.05% (m/v) Pluronic F-127 and 10 μM di-8-ANEPPS. PBMCs were isolated by density gradient using Lymphoprep and counted in a Neubauer improved hemocytometer. They were incubated at a density of 3000 cells/mL in Pluronic-supplemented buffer with 3.3 mM di-8-ANEPPS. Cells were incubated with the fluorescent probe during 1 h at room temperature, with gentle agitation, and protected from light. Unbound probe was washed with Pluronic-free buffer on two centrifugation cycles.

The maximum concentration of DMSO in the samples was % (v/v) at 7 μM of peptide. Excitation spectra and the ratio of intensities at the excitation wavelengths of 455 and 525 nm ($R = I_{455}/I_{525}$) were obtained with emission set at 670 nm to avoid membrane fluidity-related artifacts.[41,61] Excitation and emission slits for these measurements were set to 5 and 10 nm, respectively. The variation of R with the peptide concentration was analyzed by a single binding site model:[62]

$$\frac{R}{R_0} = \frac{{}^{R_{\min}}\!/_{R_0}[\text{peptide}]}{K_d + [\text{peptide}]} \quad (5)$$

with the R values normalized for R_0, the value in the absence of peptide. $R_{\min}$ defines the asymptotic minimum value of R, and K_d is the dissociation constant.

Anti-HIV Assays.

All the activities involving HIV-1 wildtype and drug-resistant strains were performed in a Biosafety Level 3 (BLS3) laboratory. The activity of test compounds against the replication of HIV-1 wt and resistant mutants in acutely infected cells was based on inhibition of virus-induced cytopathogenicity in MT-4 cells. Briefly, an amount of 50 μL of culture medium containing 1×10^4 cells was added to each well of flat-bottom microtiter trays containing 50 μL of culture medium without or with different serial concentrations of test compounds. Then, 20 μL of an HIV suspension (containing the appropriate amount of $CCID_{50}$ needed to cause complete cytopathogenicity at day 4) was added. After 96 h of incubation at 37 °C, cell viability was determined by the 3-(4,5-dimethylthiazol-1-yl)-2,5-diphenyltetrazolium bromide (MTT) method.[63] The cytotoxicity of test compounds was evaluated in parallel with their antiviral activity through the viability of mock-infected, treated cells, as monitored by the MTT method.

Data Analysis.

Fitting of the experimental data using the equations mentioned before was done by nonlinear regression using Graphpad Prism 5. Error bars on data presentation represent the standard error of the mean (SEM).

ACKNOWLEDGMENTS

This work was supported by Fundação para a Ciência e a Tecnologia − Ministério da Ciência, Tecnologia e Ensino Superior (FCT-MCTES, Portugal) grant PTDC/BBB-BQB/ 3494/2014, fellowship SPRH/BD/5243½013 to B.G., and the National Institutes of Health (NIH, USA) grant AI121349. This work was also supported by UID/BIM/ 50005/2019, a project funded by FCT-MCTES through Fundos do Orçamento do Estado. The authors thank Dr. Matteo Porotto (Department of Pediatrics and Center for Host-Pathogen Interaction, Columbia University Medical Center, New York, USA) for providing the peptide C34-HC.

REFERENCES

(1). World Health Organization (WHO). (accessed Aug 16, 2017) Global Health Observatory (GHO) data: HIV/AIDS, available from http://www.who.int/gho/hiv/en/.

(2). Harrison SC (2008) Viral membrane fusion. Nat. Struct. Mol. Biol 15 (7), 690–698. [PubMed: 18596815]

(3). Feng Y, Broder CC, Kennedy PE, and Berger EA (1996) HIV-1 entry cofactor: functional cDNA cloning of a seventransmembrane, G protein-coupled receptor. Science 272 (5263), 872–877. [PubMed: 8629022]

(4). Berger EA, Murphy PM, and Farber JM (1999) Chemokine receptors as HIV-1 coreceptors: roles in viral entry, tropism, and disease. Annu. Rev. Immunol 17, 657–700. [PubMed: 10358771]

(5). Alkhatib G, and Berger EA (2007) HIV coreceptors: from discovery and designation to new paradigms and promise. Eur. J. Med. Res 12 (9), 375–384. [PubMed: 17933717]

(6). Lakomek NA, Kaufman JD, Stahl SJ, and Wingfield PT (2014) HIV-1 envelope protein gp41: an NMR study of dodecyl phosphocholine embedded gp41 reveals a dynamic prefusion intermediate conformation. Structure 22 (9), 1311–1321. [PubMed: 25132083]

(7). Blumenthal R, Durell S, and Viard M (2012) HIV entry and envelope glycoprotein-mediated fusion. J. Biol. Chem 287 (49), 40841–40849. [PubMed: 23043104]

(8). Chan DC, Fass D, Berger JM, and Kim PS (1997) Core structure of gp41 from the HIV envelope glycoprotein. Cell 89 (2), 263–273. [PubMed: 9108481]

(9). Veiga AS, Santos NC, Loura LMS, Fedorov A, and Castanho MARB (2004) HIV fusion inhibitor peptide T-1249 is able to insert or adsorb to lipidic bilayers. Putative correlation with improved efficiency. J. Am. Chem. Soc 126 (45), 14758–14763. [PubMed: 15535700]

(10). Gallo SA, Finnegan CM, Viard M, Raviv Y, Dimitrov A, Rawat SS, Puri A, Durell S, and Blumenthal R (2003) The HIV Env-mediated fusion reaction. Biochim. Biophys. Acta 1614 (1), 36–50. [PubMed: 12873764]

(11). Wilen CB, Tilton JC, and Doms RW (2012) HIV: cell binding and entry. Cold Spring Harbor Perspect. Med 2 (8), a006866.

(12). Steffen I, and Pöhlmann S (2010) Peptide-based inhibitors of the HIV envelope protein and other class I viral fusion proteins. Curr. Pharm. Des 16 (9), 1143–1158. [PubMed: 20030613]

(13). Miyamoto F, and Kodama EN (2012) Novel HIV-1 fusion inhibition peptides: designing the next generation of drugs. Antivir. Chem. Chemother 22 (4), 151–158. [PubMed: 22182762]

(14). Tan JJ, Ma XT, Liu C, Zhang XY, and Wang CX (2013) The current status and challenges in the development of fusion inhibitors as therapeutics for HIV-1 infection. Curr. Pharm. Des 19 (10), 1810–1817. [PubMed: 23092283]

(15). LaBonte J, Lebbos J, and Kirkpatrick P (2003) Enfuvirtide. Nat. Rev. Drug Discovery 2 (5), 345–346. [PubMed: 12755128]

(16). Baldwin CE, Sanders RW, Deng Y, Jurriaans S, Lange JM, Lu M, and Berkhout B (2004) Emergence of a drug-dependent human immunodeficiency virus type 1 variant during therapy with the T20 fusion inhibitor. J. Virol 78 (22), 12428–12437. [PubMed: 15507629]

(17). Doms RW, and Trono D (2000) The plasma membrane as a combat zone in the HIV battlefield. Genes Dev 14 (21), 2677–2688. [PubMed: 11069884]

(18). Ingallinella P, Bianchi E, Ladwa NA, Wang YJ, Hrin R, Veneziano M, Bonelli F, Ketas TJ, Moore JP, Miller MD, and Pessi A (2009) Addition of a cholesterol group to an HIV-1 peptide fusion inhibitor dramatically increases its antiviral potency. Proc. Natl. Acad. Sci. U. S. A 106 (14), 5801–5806. [PubMed: 19297617]

(19). Pessi A, Langella A, Capito E, Ghezzi S, Vicenzi E, Poli G, Ketas T, Mathieu C, Cortese R, Horvat B, Moscona A, and Porotto M (2012) A General Strategy to Endow Natural Fusion-protein-Derived Peptides with Potent Antiviral Activity. PLoS One 7 (5), e36833. [PubMed: 22666328]

(20). Hollmann A, Matos PM, Augusto MT, Castanho MARB, and Santos NC (2013) Conjugation of Cholesterol to HIV-1 Fusion Inhibitor C34 Increases Peptide-Membrane Interactions Potentiating Its Action. PLoS One 8 (4), e60302. [PubMed: 23565220]

(21). Porotto M, Yokoyama CC, Palermo LM, Mungall B, Aljofan M, Cortese R, Pessi A, and Moscona A (2010) Viral entry inhibitors targeted to the membrane site of action. J. Virol 84 (13), 6760–6768. [PubMed: 20357085]

(22). Mathieu C, Augusto MT, Niewiesk S, Horvat B, Palermo LM, Sanna G, Madeddu S, Huey D, Castanho MA, Porotto L, Santos NC, and Moscona A (2017) Broad spectrum antiviral activity for paramyxoviruses is modulated by biophysical properties of fusion inhibitory peptides. Sci. Rep 7, 43610. [PubMed: 28344321]

(23). Figueira TN, Palermo LM, Veiga AS, Huey D, Alabi CA, Santos NC, Welsch JC, Mathieu C, Horvat B, Niewiesk S, Moscona A, Castanho MA, and Porotto M (2017) In Vivo Efficacy of Measles Virus Fusion Protein-Derived Peptides Is Modulated by the Properties of Self-Assembly and Membrane Residence. J. Virol 91 (1), e01554–16. [PubMed: 27733647]

(24). Chan DC, Chutkowski CT, and Kim PS (1998) Evidence that a prominent cavity in the coiled coil of HIV type 1 gp41 is an attractive drug target. Proc. Natl. Acad. Sci. U. S. A 95 (26), 15613–15617. [PubMed: 9861018]

(25). Eckert DM, and Kim PS (2001) Design of potent inhibitors of HIV-1 entry from the gp41 N-peptide region. Proc. Natl. Acad. Sci. U. S. A 98 (20), 11187–11192. [PubMed: 11572974]

(26). Armand-Ugoń M, Gutieŕrez A, Clotet B, and Este JA (2003) HIV-1 resistance to the gp41-dependent fusion inhibitor C-34. Antiviral Res 59 (2), 137–142. [PubMed: 12895697]

(27). Liu SY, Aliyari R, Chikere K, Li G, Marsden MD, Smith JK, Pernet O, Guo H, Nusbaum R, Zack JA, Freiberg AN, Su L, Lee B, and Cheng G (2013) Interferon-inducible cholesterol-25-hydroxylase broadly inhibits viral entry by production of 25-hydroxycholesterol. Immunity 38 (1), 92–105. [PubMed: 23273844]

(28). Bauman DR, Bitmansour AD, McDonald JG, Thompson BM, Liang G, and Russell DW (2009) 25-Hydroxycholesterol secreted by macrophages in response to Toll-like receptor activation suppresses immunoglobulin A production. Proc. Natl. Acad. Sci. U. S. A 106 (39), 16764–16769. [PubMed: 19805370]

(29). Cyster JG, Dang EV, Reboldi A, and Yi T (2014) 25-Hydroxycholesterols in innate and adaptive immunity. Nat. Rev. Immunol 14 (11), 731–743. [PubMed: 25324126]

(30). Li C, Deng YQ, Wang S, Ma F, Aliyari R, Huang XY, Zhang NN, Watanabe M, Dong HL, Liu P, Li XF, Ye Q, Tian M, Hong S, Fan J, Zhao H, Li L, Vishlaghi N, Buth JE, Au C, Liu Y, Lu N, Du P, Qin FX, Zhang B, Gong D, Dai X, Sun R, Novitch BG, Xu Z, Qin CF, and Cheng G (2017) 25-Hydroxycholesterol Protects Host against Zika Virus Infection and Its Associated Microcephaly in a Mouse Model. Immunity 46 (3), 446–456. [PubMed: 28314593]

(31). Westover EJ, and Covey DF (2006) Synthesis of ent-25-hydroxycholesterol. Steroids 71 (6), 484–488. [PubMed: 16519912]

(32). Gomes B, Gonçalves S, Disalvo A, Hollmann A, and Santos NC (2018) Effect of 25-hydroxycholesterol in viral membrane fusion: Insights on HIV inhibition. Biochim. Biophys. Acta 1860 (5), 1171–1178.

(33). Desmezieres E, Gupta N, Vassell R, He Y, Peden K, Sirota L, Yang Z, Wingfield P, and Weiss CD (2005) Human immunodeficiency virus (HIV) gp41 escape mutants: cross-resistance to peptide inhibitors of HIV fusion and altered receptor activation of gp120. J. Virol 79 (8), 4774–4781. [PubMed: 15795263]

(34). Augusto MT, Hollmann A, Castanho MARB, Porotto M, Pessi A, and Santos NC (2014) Improvement of HIV fusion inhibitor C34 efficacy by membrane anchoring and enhanced exposure infection. J. Antimicrob. Chemother 69, 1286–1297. [PubMed: 24464268]

(35). Gomes B, Porotto M, and Santos NC (2017) Biophysical properties and antiviral activities of measles fusion protein derived peptide conjugated with 25-hydroxycholesterol. Molecules 22 (11), 1869.

(36). Popik W, Alce TM, and Au W (2002) Human immunodeficiency virus type 1 uses lipid raft-colocalized CD4 and chemokine receptors for productive entry into CD4(+) T cells. J. Virol 76 (10), 4709–4722. [PubMed: 11967288]

(37). Mañes S, del Real G, Lacalle RA, Lucas P, Goṁez-Moutoń C, Sańchez-Palomino S, Delgado R, Alcamí J, Mira E, and Martínez-A C (2000) Membrane raft microdomains mediate lateral assemblies required for HIV-1 infection. EMBO Rep 1 (2), 190–196. [PubMed: 11265761]

(38). Huarte N, Carravilla P, Cruz A, Lorizate M, Nieto-Garai JA, Kraüsslich HG, Peŕez-Gil J, Requejo-Isidro J, and Nieva JL (2016) Functional organization of the HIV lipid envelope. Sci. Rep 6, 34190. [PubMed: 27678107]

(39). Franquelim HG, Loura LMS, Santos NC, and Castanho MARB (2008) Sifuvirtide screens rigid membrane surfaces. Establishment of a correlation between efficacy and membrane domain selectivity among HIV fusion inhibitor peptides. J. Am. Chem. Soc 130 (19), 6215–6223. [PubMed: 18410103]

(40). Fernandes MX, García de la Torre J, and Castanho MARB (2002) Joint determination by Brownian dynamics and fluorescence quenching of the in-depth location profile of biomolecules in membranes. Anal. Biochem 307 (1), 1–12. [PubMed: 12137772]

(41). Gross E, Bedlack RS, and Loew LM (1994) Dual-wavelength ratiometric fluorescence measurement of the membrane dipole potential. Biophys. J 67 (1), 208–216. [PubMed: 7918989]

(42). Matos PM, Franquelim HG, Castanho MARB, and Santos NC (2010) Quantitative assessment of peptide-lipid interactions. Ubiquitous fluorescence methodologies. Biochim. Bio-phys. Acta 1798 (11), 1999–2012.

(43). Beck Z, Brown BK, Wieczorek L, Peachman KK, Matyas GR, Polonis VR, Rao M, and Alving CR (2009) Human erythrocytes selectively bind and enrich infectious HIV-1 virions. PLoS One 4 (12), e8297. [PubMed: 20011536]

(44). He W, Neil S, Kulkarni H, Wright E, Agan BK, Marconi VC, Dolan MJ, Weiss RA, and Ahuja SK (2008) Duffy antigen receptor for chemokines mediates trans-infection of HIV-1 from red blood cells to target cells and affects HIV-AIDS susceptibility. Cell Host Microbe 4 (1), 52–62. [PubMed: 18621010]

(45). Hess C, Klimkait T, Schlapbach L, Del Zenero V, Sadallah S, Horakova E, Balestra G, Werder V, Schaefer C, Battegay M, and Schifferli JA (2002) Association of a pool of HIV-1 with erythrocytes in vivo: a cohort study. Lancet 359 (9325), 2230–2234. [PubMed: 12103286]

(46). Leidl K, Liebisch G, Richter D, and Schmitz G (2008) Mass spectrometric analysis of lipid species of human circulating blood cells. Biochim. Biophys. Acta, Mol. Cell Biol. Lipids 1781 (10), 655–664.

(47). He Y, Liu S, Li J, Lu H, Qi Z, Liu Z, Debnath AK, and Jiang S (2008) Conserved salt bridge between the N-and C-terminal heptad repeat regions of the human immunodeficiency virus type 1 gp41 core structure is critical for virus entry and inhibition. J. Virol 82, 11129–39. [PubMed: 18768964]

(48). Stanford University. (accessed Feb 9, 2019) HIV Drug Resistance Database, available from https://hivdb.stanford.edu/.

(49). El-Brollosy NR, Al-Deeb OA, El-Emam AA, Pedersen EB, La Colla P, Collu G, Sanna G, and Loddo R (2009) Synthesis of novel uracil non-nucleoside derivatives as potential reverse transcriptase inhibitors of HIV-1. Arch. Pharm 342 (11), 663–70.

(50). Mayer LD, Hope MJ, and Cullis PR (1986) Vesicles of variable sizes produced by a rapid extrusion procedure. Biochim. Biophys. Acta 858 (1), 161–168. [PubMed: 3707960]

(51). Szoka F, Olson F, Heath T, Vail W, Mayhew E, and Papahadjopoulos D (1980) Preparation of unilamellar liposomes of intermediate size (0.1–0.2 μmol) by a combination of reverse phase evaporation and extrusion through polycarbonate membranes. Biochim. Biophys. Acta 601 (3), 559–571. [PubMed: 6251878]

(52). Kubista M, Sjoback R, Eriksson S, and Albinsson B (1994) Experimental correction for the inner-filter effect in fluorescence spectra. Analyst 119 (3), 417.

(53). Santos NC, Prieto M, and Castanho MARB (2003) Quantifying molecular partition into model systems of biomembranes: An emphasis on optical spectroscopic methods. Biochim. Biophys. Acta 1612 (2), 123–135. [PubMed: 12787930]

(54). Chiu SW, Subramaniam S, and Jakobsson E (1999) Simulation study of a gramicidin/lipid bilayer system in excess water and lipid. II. Rates and mechanisms of water transport. Biophys. J 76, 1929–1938. [PubMed: 10096891]

(55). Greenwood AI, Tristram-Nagle S, and Nagle JF (2006) Partial molecular volumes of lipids and cholesterol. Chem. Phys. Lipids 143 (1–2), 1–10. [PubMed: 16737691]

(56). Yamazaki M, Miyazu M, Asano T, Yuba A, and Kume N (1994) Direct evidence of induction of interdigitated gel structure in large unilamellar vesicles of dipalmitoylphosphatidylcholine by ethanol: studies by excimer method and high-resolution electron cryomicroscopy. Biophys. J 66, 729–733. [PubMed: 8011904]

(57). Santos NC, Prieto M, and Castanho MA (1998) Interaction of the major epitope region of HIV protein gp41 with membrane model systems. A fluorescence spectroscopy study. Biochemistry 37, 8674–8682. [PubMed: 9628729]

(58). Nagle JF, and Wiener MC (1988) Structure of fully hydrated bilayer dispersions. Biochim. Biophys. Acta 942 (1), 1–10. [PubMed: 3382651]

(59). Matos PM, Castanho MARB, and Santos NC (2010) HIV-1 fusion inhibitor peptides enfuvirtide and T-1249 interact with erythrocyte and lymphocyte membranes. PLoS One 5 (3), e9830. [PubMed: 20352107]

(60). Matos PM, Freitas T, Castanho MARB, and Santos NC (2010) The role of blood cell membrane lipids on the mode of action of HIV-1 fusion inhibitor sifuvirtide. Biochem. Biophys. Res. Commun 403 (3–4), 270–274. [PubMed: 21075080]

(61). Clarke RJ, and Kane DJ (1997) Optical detection of membrane dipole potential: avoidance of fluidity and dye-induced effects. Biochim. Biophys. Acta 1323 (2), 223–239. [PubMed: 9042345]

(62). Cladera J, and O'Shea P (1998) Intramembrane molecular dipoles affect the membrane insertion and folding of a model amphiphilic peptide. Biophys. J 74 (5), 2434–2442. [PubMed: 9591669]

(63). Pauwels R, Balzarini J, Baba M, Snoeck R, Schols D, Herdewijn P, Desmyter J, and De Clercq E (1988) Rapid and Automated Tetrazolium-Based Colorimetric Assay for the Detection of Anti-HIV Compounds. J. Virol. Methods 20, 309–321. [PubMed: 2460479]

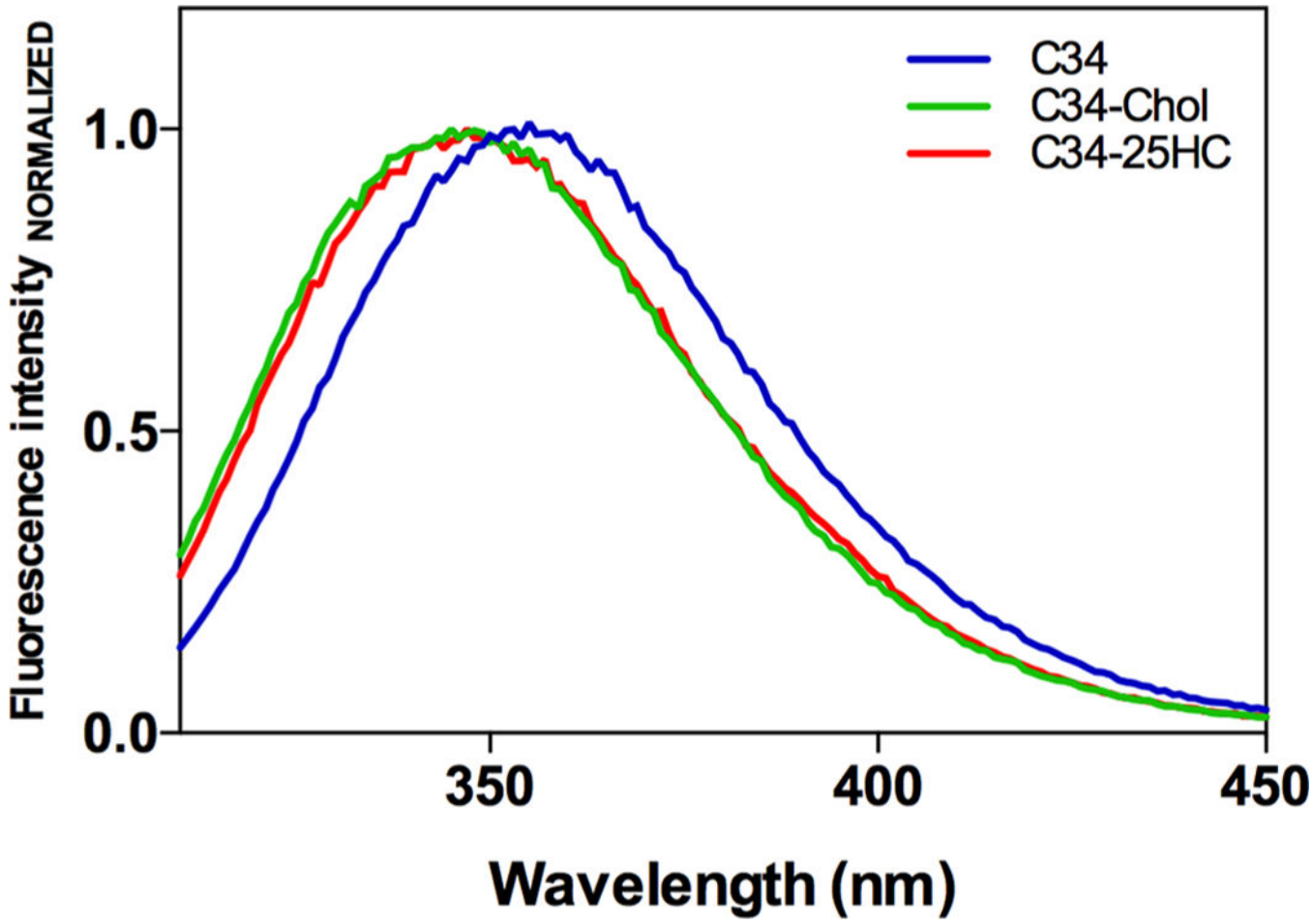

Figure 1.
Normalized fluorescence emission spectra of 5 mM C34, C34-cholesterol, and C34-HC in aqueous solution (λ_{exc} = 280 nm).

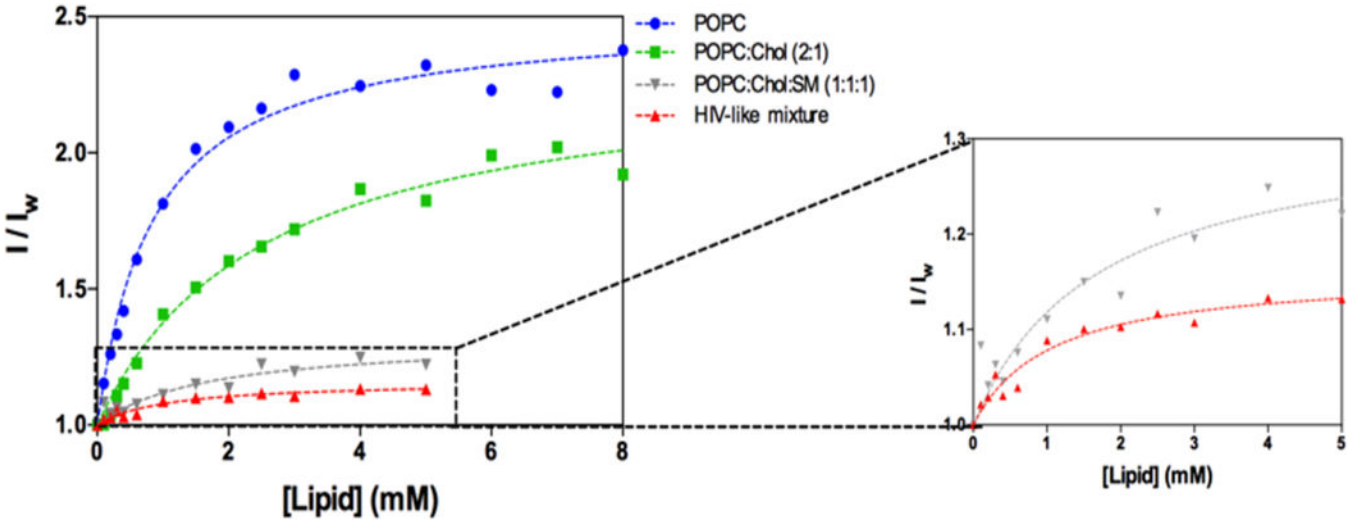

Figure 2.

Partition of C34-HC to lipid vesicles. Evaluation of the Trp fluorescence variations of 5 μM C34-HC upon titration with POPC, POPC:Chol (2:1), POPC:Chol:SM (1:1:1), or an HIV-like mixture with an LUV suspension. Dashed lines are fittings of experimental data using eq 1.

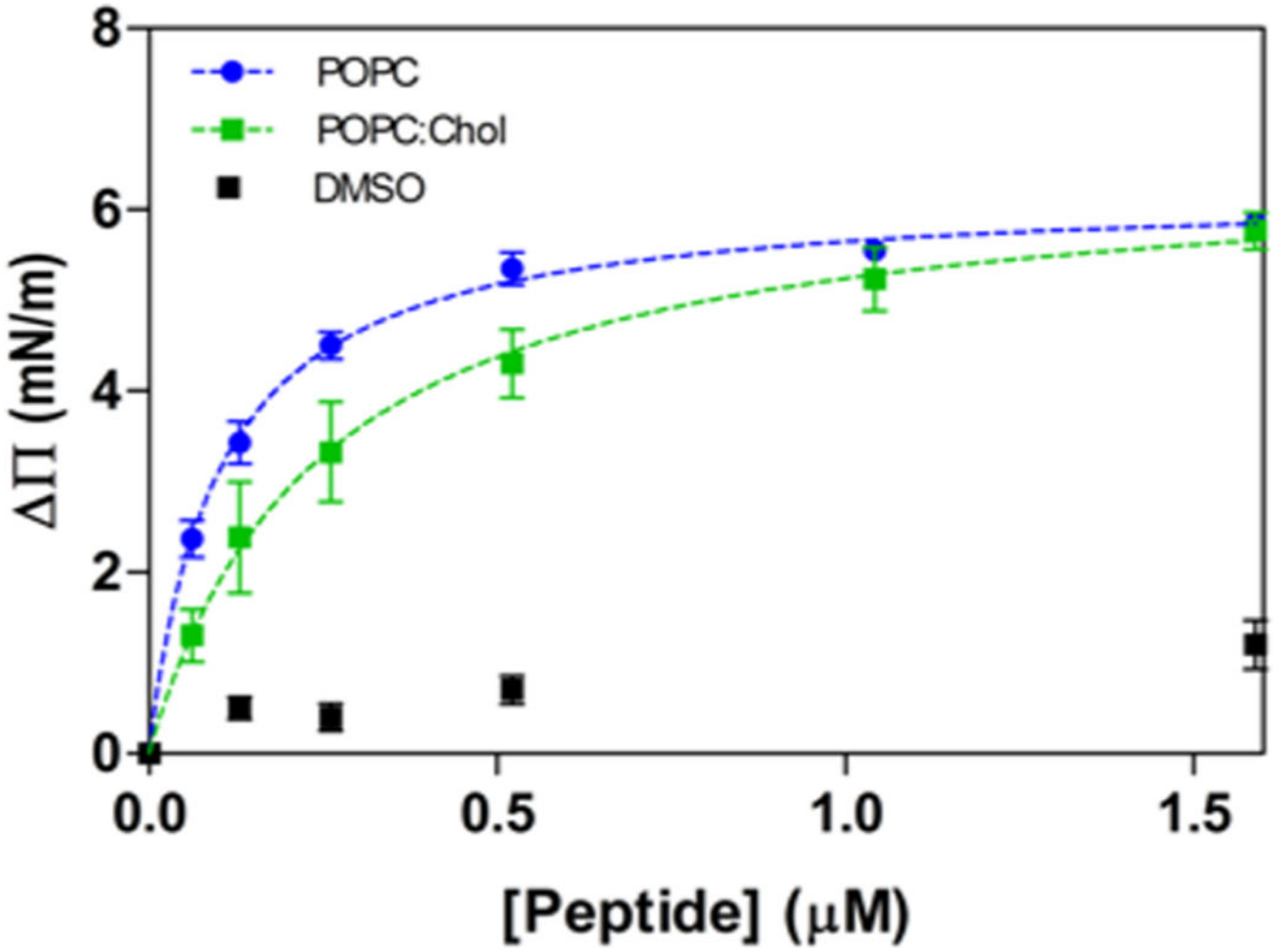

Figure 3.

Interaction of C34-HC with lipid monolayers. Changes in surface pressure as a function of C34-HC addition to pure POPC and POPC:Chol 2:1. Dashed lines were obtained by fitting experimental data using eq 2.

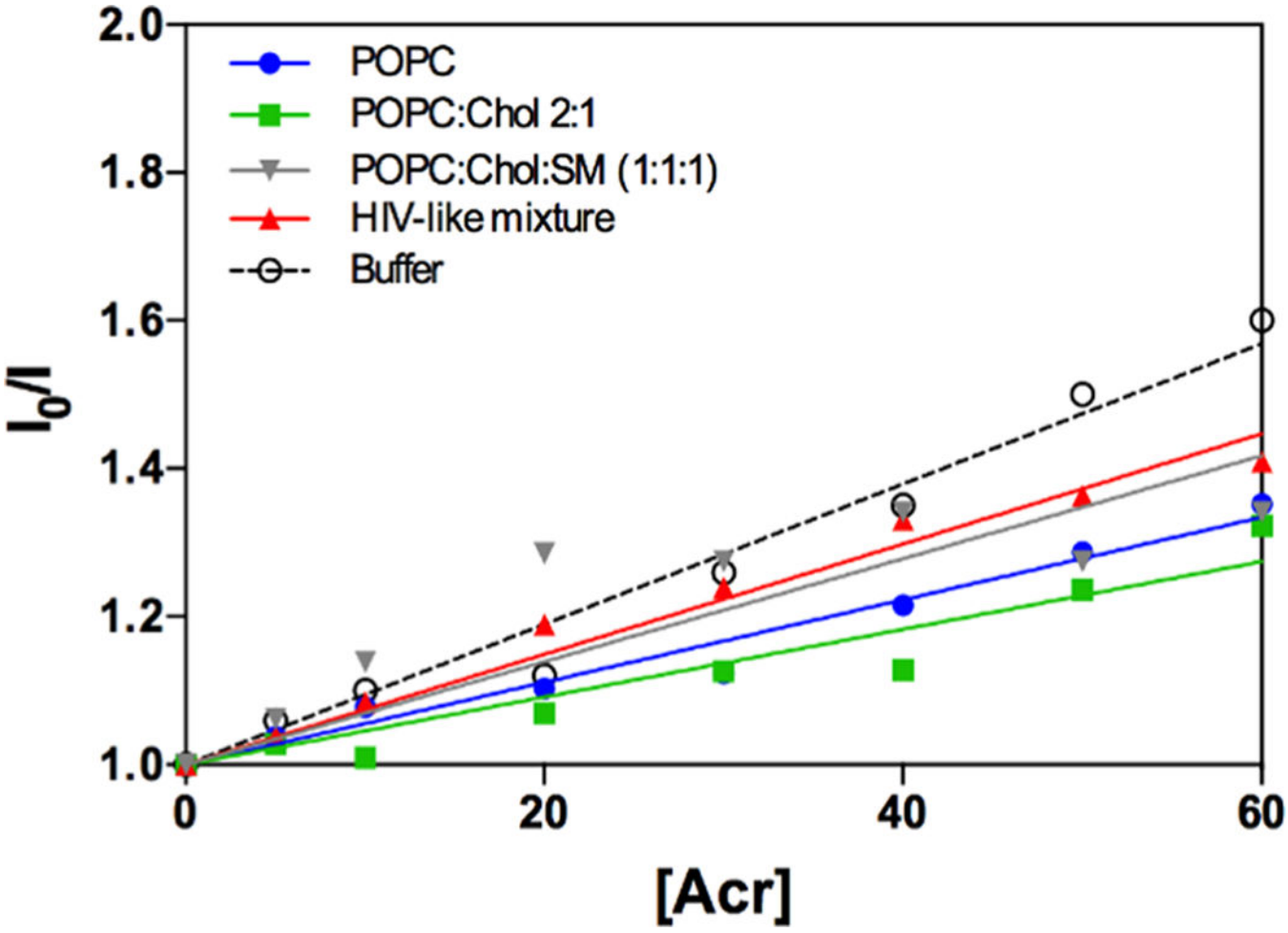

Figure 4.

Accessibility of the peptide to the aqueous medium. Fluorescence quenching of C34-HC by acrylamide, in the presence of buffer or lipid vesicles. Lipid compositions tested were pure POPC, POPC:Chol (2:1), POPC:Chol:SM (1:1:1), and an HIV-like mixture. Lines are fittings of experimental data using the Stern−Volmer equation (eq 3).

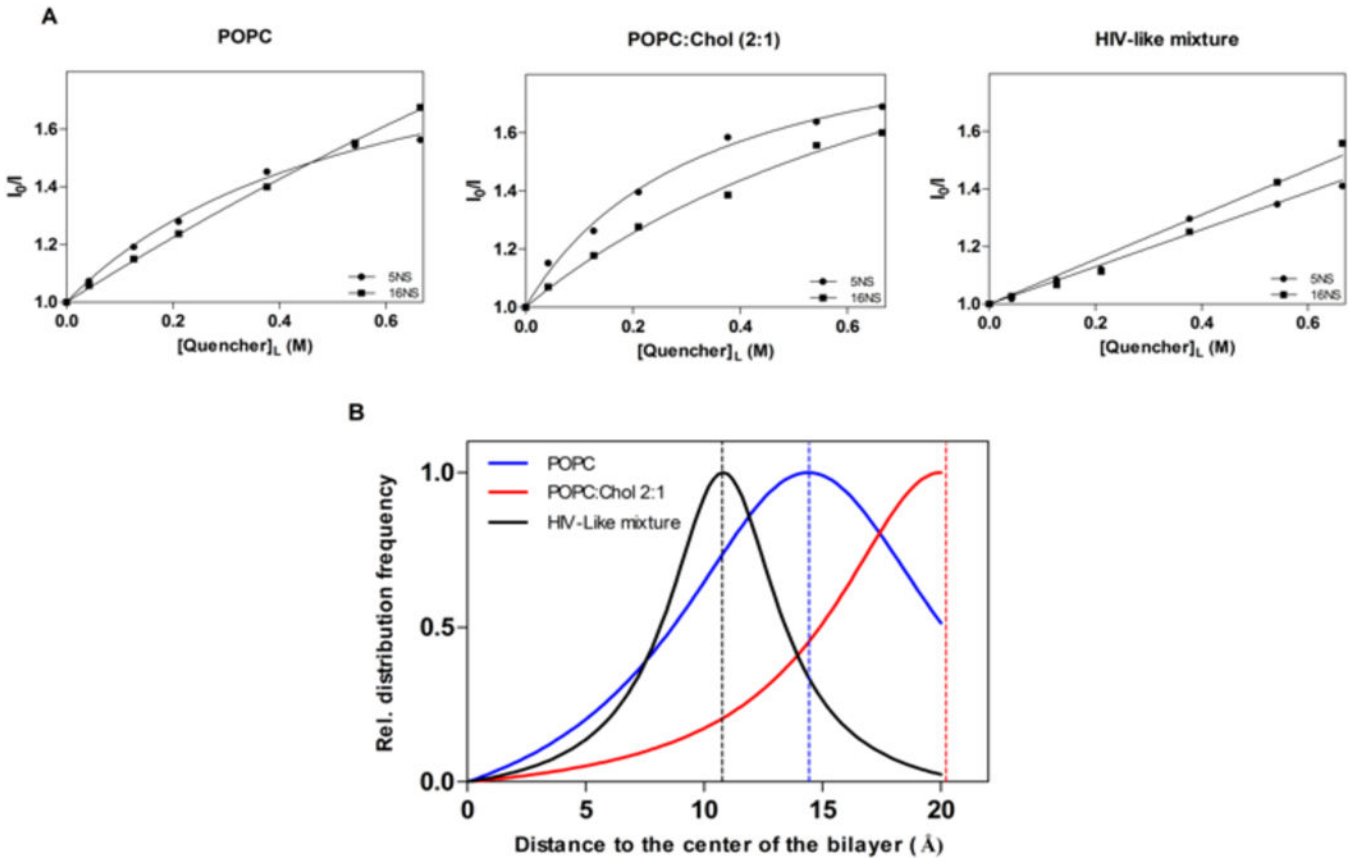

Figure 5.

Localization of C34-HC in the bilayer. (A) Stern−Volmer plots for the quenching of C34-HC fluorescence by 5NS or 16NS in POPC, POPC:Chol 2:1, and the HIV-like mixture with LUVs, obtained using time-resolved fluorescence measurements. Each point is the average of three independent measures. The dashed lines are fittings of the experimental data using the Lehrer equation (eq 4). (B) Depth of insertion of C34-HC Trp residues in the referred membranes, calculated using the SIMEXDA method,[40] yielding an average location 15 Å away from the center of the bilayer for POPC, 20 Å for POPC:Chol 2:1, and 11 Å for the HIV-like mixture.

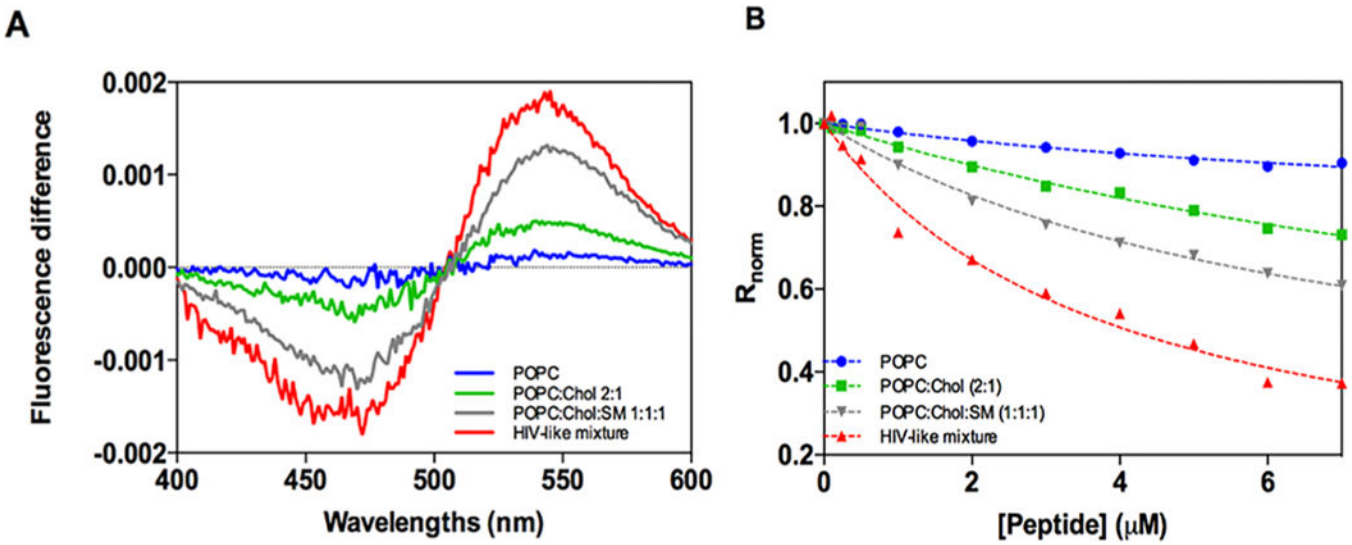

Figure 6.

C34-HC interaction with di-8-ANEPPS labeled LUVs. (A) Differential spectra of di-8-ANEPPS bound to LUVs with different lipid composition in the presence of C34-HC and in its absence. Spectra were obtained by subtracting the excitation spectrum (normalized to the integrated areas) of labeled vesicles in the absence of peptide from the spectrum in the presence of peptide (7 μM). (B) Binding profiles of C34-HC to vesicles of POPC, POPC:Chol 2:1, POPC:Chol:SM 1:1:1, and the HIV-like mixture, obtained by plotting the di-8-ANEPPS excitation ratio, R (I_{455}/I_{525}, normalized to the initial value), as a function of the peptide concentration.

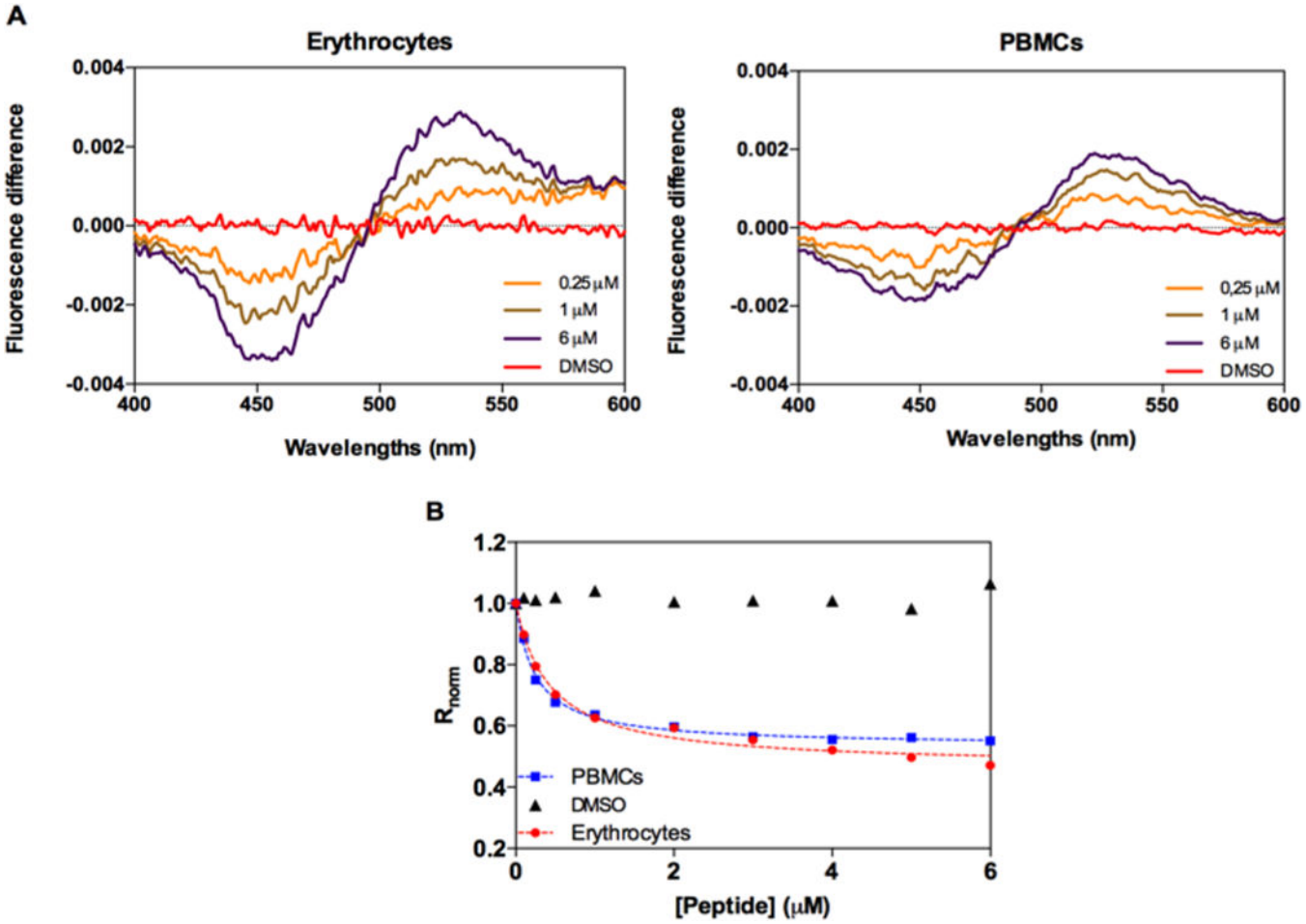

Figure 7.

C34-HC interactions with di-8-ANEPPS labeled cells. (A) Differential spectra of di-8-ANEPPS bound to erythrocytes and PBMCs in the presence of C34-HC and in its absence. Spectra were obtained by subtracting the excitation spectrum (normalized to the integrated areas) of labeled vesicles in the absence of peptide from the spectrum in the presence of the peptide (different concentrations). (B) Binding profiles of C34-HC to erythrocytes and PBMCs by plotting the di-8-ANEPPS excitation ratio, R (I_{455}/I_{525}), normalized to the initial value, as a function of the peptide concentration.

Table 1.

Partition Coefficients[a]

lipid mixture	K_p	I_L/I_W
POPC	1543 ± 347	2.50 ± 0.09
POPC:Chol (2:1)	516 ± 90	2.33 ± 0.09
POPC:Chol:SM (1:1:1)	775 ± 307	1.31 ± 0.05
HIV-like mixture	1245 ± 297	1.16 ± 0.04

[a]Parameters obtained from the fitting of the fluorescence data of the partition assays of 5 μM C34-HC using eq 1. All measures were made at least in triplicate. Values are presented as mean ± standard error of mean (SEM).

Table 2.

Membrane Dipole Potential Experiments with LUVs[a]

lipid composition	K_d	R_{min}
POPC	11.0 ± 7.7	−0.27 ± 0.13
POPC:Chol (2:1)	14.3 ± 8.2	−0.83 ± 0.35
POPC:Chol:SM (1:1:1)	7.10 ± 5.3	−0.79 ± 0.35
HIV-like mixture	3.91 ± 1.6	−0.97 ± 0.18

[a]Parameters obtained from the fitting of the fluorescence data of the interaction of C34-HC different vesicles with different lipid composition using eq 5. All measurements were made at least in triplicate. Values are presented as mean ± standard error of mean.

Table 3.

Cytotoxicity and *in Vitro* Antiviral Activity of C34-HC and Enfuvirtide against HIV-1 Wild-Type ($HIV\text{-}1_{IIIB}$), NNRTI-Resistant Strains (N119, A17, and EFVR), and an NRTI-Resistant Strain (AZTR)[a]

	MT-4	HIV-1_{IIIB}	N119 (Y181C)	A17 (K103N, Y181C)	EFV^R (K103R, V179D, P225H)	AZT^R (67N, 70R, 215F, 219Q)
peptide	CC 50[b] (nM)	IC_{90}[c] (nM)	IC_{50}[c] (nM)			
C34-HC	2200	2	0.8	0.7	0.7	0.8	0.9
enfuvirtide	>22 000	80	20	19	15	18	20

[a]Data represent mean values ± SD for three independent determinations. For values where SD is not shown, variation among triplicate samples was less than 15%.

[b]Compound concentration required to reduce the viability of mock-infected MT-4 cells by 50%, as determined by the 3-(4,5-dimethylthiazol-1-yl)-2,5-diphenyltetrazolium bromide (MTT) method.

[c]Compound concentration required to achieve 90% or 50% protection of MT-4 cells from HIV-1 induced cytopathogenicity, as determined by the MTT method.